

**CHARACTERISATION AND  
CRYSTALLISATION OF DEPTOR**

**YEAP KEAN HENG**

**UNIVERSITI SAINS MALAYSIA**

**2021**

# **CHARACTERISATION AND CRYSTALLISATION OF DEPTOR**

by

**YEAP KEAN HENG**

**Thesis submitted in fulfilment of the requirements  
for the degree of  
Master of Science**

**February 2021**

## **ACKNOWLEDGEMENT**

I would like to acknowledge everyone who played a role in my studies. Firstly, I wish to convey my sincere thanks to my supervisor Dr Teh Aik Hong, for his guidance and constructive comments regarding my laboratory tasks throughout my journey. Secondly, I also owe many thanks to my lab members for invigorating discussions and great opinions regarding my work during my studies. Finally, I would like to give my special gratitude to my family members for their encouragement, helpful staff members and to MyMaster program for their financial support.

## TABLE OF CONTENTS

<b>ACKNOWLEDGEMENT</b> .....	<b>ii</b>
<b>TABLE OF CONTENTS</b> .....	<b>iii</b>
<b>LIST OF TABLES</b> .....	<b>vi</b>
<b>LIST OF FIGURES</b> .....	<b>vii</b>
<b>LIST OF ABBREVIATIONS</b> .....	<b>vii</b>
<b>ABSTRAK</b> .....	<b>xii</b>
<b>ABSTRACT</b> .....	<b>xiv</b>
<b>CHAPTER 1 INTRODUCTION</b> .....	<b>1</b>
1.1 Introduction .....	1
1.2 Research Objectives .....	2
<b>CHAPTER 2 LITERATURE REVIEW</b> .....	<b>3</b>
2.1 mTOR.....	3
2.1.1 Structure of mTOR.....	4
2.1.1(a) FAT domain.....	5
2.1.1(b) Kinase domain.....	6
2.2 DEPTOR .....	7
2.2.1 Biological functions of DEPTOR .....	7
2.2.2 DEPTOR regulation.....	8
2.2.3 DEP domain .....	9
2.2.4 PDZ domain .....	11
2.3 X-ray protein crystallography .....	12
<b>CHAPTER 3 MATERIALS AND METHODS</b> .....	<b>14</b>
3.1 Cloning by homologous recombination method .....	14
3.1.1 Polymerase Chain Reaction (PCR).....	14
3.1.2 Restriction Enzyme Digestion .....	15

3.1.3	DNA Purification .....	15
3.1.4	Agarose Gel Electrophoresis.....	16
3.1.5	Cloning of DEPTOR and its truncated mutants into pET-21a(+)..	16
3.1.6	Correcting mutation at position 611 and 1166.....	18
3.1.7	Identification and optimization of rare codons in DEPTOR.....	19
3.2	General transformation of <i>E. coli</i> for cloning .....	21
3.2.1	Transformation of <i>E. coli</i> with recombinant vector for expression	21
3.2.2	Transformation of <i>E. coli</i> with rare tRNA-supplying plasmid .....	22
3.2.3	Transformation of NiCo21(DE3)-tRNA plasmid with recombinant vector.....	22
3.3	Colony PCR and plasmid isolation .....	22
3.4	Protein expression .....	23
3.4.1	Small-scale protein expression using recombinant pET-21a(+)	23
3.4.2	Small-scale expression of DEPTOR in NiCo21(DE3) .....	24
3.4.3	Small-scale expression of DEPTOR with rare tRNA-supplying plasmid.....	24
3.4.4	Large-scale Protein expression using recombinant pET-21a(+)	25
3.4.5	Cell lysis and protein extraction.....	25
3.5	Protein purification.....	26
3.5.1	Immobilized Metal-Ion Affinity Chromatography (IMAC) .....	26
3.5.2	SEC .....	27
3.5.2(a)	Molecular weight determination.....	27
3.5.3	Nickel affinity test.....	28
3.5.4	Bradford protein assay .....	29
3.5.5	Sodium Dodecyl Sulfate Polyacrylamide Gel Electrophoresis (SDS-PAGE).....	29
3.6	Liquid Chromatography Mass Spectrometry (LC-MS) .....	30
3.7	Dynamic light scattering .....	30

3.8	Protein crystallisation experiments .....	30
3.9	Homology modelling of DEPTOR.....	40
<b>CHAPTER 4 RESULTS .....</b>		<b>42</b>
4.1	Cloning of DEPTOR into pET-21a(+)	42
4.1.1	Mutations correction at Ser204 and Asn389.....	43
4.1.2	Codon optimization of DEPTOR.....	44
4.1.3	Cloning of DEPTOR's truncated mutants into pET-21a(+)	47
4.2	Cloning of kinase domains and FAT domains of mTOR into pET-21a(+)	49
4.3	Small scale expression of DEPTOR.....	49
4.3.1	Optimization of DEPTOR expression.....	50
4.3.2	Expression of DEPTOR with rare tRNA supplementation in NiCo21(DE3)	53
4.3.3	Small Scale expression of DEPTOR mutants .....	55
4.4	Expression of kinase domains and FAT domains .....	57
4.5	Large scale protein expression .....	57
4.6	Protein identification by LC-MS.....	62
4.7	Dynamic light scattering (DLS) .....	62
4.8	Protein crystallisation.....	66
4.8.1	DEPTOR crystallisation.....	66
4.8.1(a)	Optimization of DEPTOR crystallisation.....	68
4.8.2	DEP12 crystallisation.....	70
4.8.2(a)	Optimization of DEP12 crystallisation.....	71
4.9	Homology Modelling of DEPTOR .....	74
<b>CHAPTER 5 DISCUSSION .....</b>		<b>78</b>
<b>CHAPTER 6 CONCLUSIONS .....</b>		<b>84</b>
<b>REFERENCES.....</b>		<b>85</b>
<b>APPENDICES</b>		

## LIST OF TABLES

	<b>Page</b>
Table 3.1	Reaction components used for plasmid DNA digestion ..... 15
Table 3.2	Primers used in the cloning of DEPTOR and its truncated mutants..... 17
Table 3.3	List of primers used to correct the mutations..... 18
Table 3.4	Nucleotide corrections by their respective primers..... 18
Table 3.5	Position of rare codons and their corresponding amino acids..... 20
Table 3.6	Lists of primers used to optimize the rare codons in DEPTOR..... 20
Table 3.7	Rare codon optimization by their respective primers. .... 20
Table 3.8	Summary of conditions used to optimize DEPTOR crystallisations at 20°C..... 33
Table 3.9	Summary of conditions used to optimize DEPTOR crystallisations at 4°C..... 35
Table 3.10	Summary of conditions used to optimize DEPTOR crystallisations at 25°C..... 35
Table 3.11	Summary of conditions used to optimize DEP12 crystallisations at 4°C..... 36
Table 3.12	Summary of additives conditions used to optimize DEP12 crystallisations at 4°C..... 39
Table 4.1	Elution volume and estimated molecular weight based on the size-exclusion profiles..... 62

## LIST OF FIGURES

	<b>Page</b>
Figure 2.1	Linear schematic of mTOR structure (1-2549 aa) .....5
Figure 2.2	Schematic structure of DEPTOR .....7
Figure 3.1	Correcting mutation at position 611 and 1166 via PCR ..... 19
Figure 3.2	Optimization of rare codons via PCR .....21
Figure 3.3	Diagram of vapour diffusion method.....32
Figure 4.1	PCR amplification of DEPTOR gene and colony PCR analysis .....42
Figure 4.2	Correction of mutations through PCR.....44
Figure 4.3	Codon optimization of DEPTOR gene via PCR. Lane M is the generuler 1kb DNA ladder .....46
Figure 4.4	Schematic structure of DEPTOR and its truncated domains .....47
Figure 4.5	PCR amplifications of truncated DEPTOR domains and colony PCR analysis .....48
Figure 4.6	SDS-PAGE analysis of recombinant DEPTOR expression.....50
Figure 4.7	SDS-PAGE analysis for expression of DEPTOR at varying IPTG concentrations at 20°C for 16 hours.....51
Figure 4.8	SDS-PAGE analysis for expression of DEPTOR at varying IPTG concentrations at 25°C for 12 hours.....52
Figure 4.9	SDS-PAGE analysis for expression of DEPTOR at varying IPTG concentrations at 30°C for 6 hours.....52
Figure 4.10	SDS-PAGE analysis for expression of DEPTOR in the presence of rare tRNA-supplying plasmid.....54
Figure 4.11	SDS-PAGE analysis for expression of DEPTOR between BL21(DE3) without any rare tRNA-supplying plasmid and Nico21 DE3 with pACYC-RIL plasmid.....54
Figure 4.12	SDS-PAGE analysis for expression of DEP1 and DEP2 (arrows) ....55



Figure 4.13	SDS-PAGE analysis for expression of DEP12 (arrow) at 0.5 mM IPTG in 25°C for 16 hours.....	56
Figure 4.14	SDS-PAGE analysis for expression of PDZ domain (arrow) at 0.5 mM IPTG in 25°C for 16 hours .....	56
Figure 4.15	SDS-PAGE analysis of purified DEPTOR by IMAC.....	58
Figure 4.16	Final purification of DEPTOR by SEC. (A) Size-exclusion profile of DEPTOR .....	58
Figure 4.17	SDS-PAGE analysis of purified DEP12 by IMAC.....	59
Figure 4.18	Final purification of DEP12 by SEC.....	59
Figure 4.19	SDS-PAGE analysis of purified DEP1 by IMAC.....	60
Figure 4.20	Final purification of DEP1 by SEC.....	60
Figure 4.21	SDS-PAGE analysis of purified DEP2 by IMAC.....	61
Figure 4.22	Final purification of DEP1 by SEC.....	61
Figure 4.23	Dynamic light scattering of DEPTOR .....	63
Figure 4.24	Dynamic light scattering of DEP1+2.....	64
Figure 4.25	Dynamic light scattering of DEP1 .....	65
Figure 4.26	Dynamic light scattering of DEP2 .....	66
Figure 4.27	Crystal (arrow) of DEPTOR formed in 0.1 M Tris pH 8.5, 0.2 M ammonium phosphate monobasic, 50% MPD at a protein concentration of 10 mg/mL.....	67
Figure 4.28	Needle-like crystals of DEPTOR formed in 0.1 M Tris-HCl pH 8.5, 0.2 M lithium sulfate monohydrate, 30% PEG 8K at a protein concentration of 10 mg/mL.....	67
Figure 4.29	Needle-like crystals of DEPTOR formed in 0.1 M sodium cacodylate trihydrate pH 6.5, magnesium acetate tetrahydrate, 20% PEG 8K at a protein concentration of 10 mg/mL.....	68
Figure 4.30	Crystal (arrows) for DEPTOR obtained during pH optimization at 20°C for crystallisation condition; 0.1 M Tris pH 8.5, 0.2 M ammonium phosphate monobasic, 50% MPD.....	69

Figure 4.31	Small hairy needle-like crystals (arrow) for DEPTOR obtained during pH optimization at 25°C for crystallisation condition; 0.1 M Tris pH 7.0, 0.2 M ammonium phosphate monobasic, 50% MPD at a protein concentration of 10 mg/mL. ....	70
Figure 4.32	Needle-like crystals (arrow) for DEP12 formed in 0.1 M HEPES pH 7.5, 10% PEG 8K, 8% ethylene glycol at a protein concentration of 10 mg/mL.....	71
Figure 4.33	Needle-like crystals of DEP12 formed in 0.1 M Tris pH 7.0, 10% PEG 8K and 8% ethylene glycol at a protein concentration of 10 mg/mL.....	72
Figure 4.34	Needle-like crystals of DEP12 formed in 0.1 M Tris pH 7.0, 10% PEG 8K at a protein concentration of 10 mg/mL .....	72
Figure 4.35	Needle-like crystals of DEP12 formed in 0.1 M Tris pH 7.0, 10% PEG 8K, 15% ethylene glycol at a protein concentration of 10 mg/mL.....	73
Figure 4.36	The parent well (0.1 M Tris pH 7.0, 10% PEG 8K, 13% ethylene glycol) containing short needle-like crystals that can be observed more clearly after some of its crystals were taken away by seeding wand for seeding purposes.....	74
Figure 4.37	Sequence alignments of DEPTOR's DEP1 and RGS7 .....	75
Figure 4.38	Homology model of DEPTOR's DEP1 region .....	75
Figure 4.39	Sequence alignments of DEPTOR's DEP2 and Pleckstrin2.....	76
Figure 4.40	Homology model of DEPTOR's DEP2 region .....	76
Figure 4.41	Sequence alignments of DEPTOR's PDZ and Shank1 .....	77
Figure 4.42	Homology model of DEPTOR's PDZ region .....	77
Figure 5.1	Schematic drawing of DEPTOR-mTOR complex.....	81

## LIST OF ABBREVIATIONS

kDa	Kilodalton
aa	Amino acids
°C	Degree Celsius
bp	Base pairs
g	Gram
M	Molar
L	Liter
mL	Milliter
mg	Milligram
ng	Nanogram
μL	Microliter
μg	Microgram
mM	Millimolar
NaCl	Sodium chloride
ddH <sub>2</sub> O	Distilled water
PCR	Polymerase chain reaction

## LIST OF APPENDICES

- Appendix A Cloning of kinase domain of mTOR into pET-21a(+)
- Appendix B Cloning of FAT domain and its truncated mutants into pET-21a(+)
- Appendix C Expression of truncated kinase domains
- Appendix D Expression of FAT domains
- Appendix E Gene Sequence of DEPTOR (*Homo Sapiens*)
- Appendix F Mutation correction of DEPTOR
- Appendix G Optimization of rare codons in DEPTOR
- Appendix H Gene sequence of DEP1
- Appendix I Gene sequence of DEP2
- Appendix J Gene sequence of DEP12
- Appendix K Gene sequence of PDZ
- Appendix L Bradford protein assay
- Appendix M Size exclusion calibration curve
- Appendix N DEPTOR identification by LCMS
- Appendix O pET-21a(+) sequence and plasmid map
- Appendix P Plasmid map of pRK5 FLAG human DEPTOR

## PENCIRIAN DAN PENGHABLURAN DEPTOR

### ABSTRAK

Sasaran mekanisme jalur isyarat rapamycin (mTOR) mengintegrasikan pelbagai jenis nutrien untuk mengatur proses selular penting yang berkaitan dengan pertumbuhan sel. mTOR adalah protein kinase serine / threonine yang besar dan wujud dalam dua kompleks yang berbeza, mTORC1 dan mTORC2. DEPTOR adalah perencat endogen mTOR dan terdiri daripada dua domain DEP dalam susunan tandem dan domain PDZ. Sistem ekspresi *Escherichia coli* digunakan untuk eksperimen pengklonan dan ekspresi eksperimen. Di sini, selain protein panjang penuh, pelbagai mutan terpotong juga dikaji untuk mendapatkan gambaran mengenai ciri dan seni bina protein. Empat mutan terpotong dibina untuk mewakili domain DEP pertama (DEP1), domain DEP kedua (DEP2), kedua domain DEP (DEP12) dan domain PDZ. DEPTOR, DEP1, DEP2 dan DEP12 telah diekspresikan sebagai protein larut tetapi PDZ sebagai tidak larut. Protein larut ditulenkan hingga kehomogenan untuk penghabluran melalui penulenan afiniti ion-logam dan kromatografi penurasan gel. Kit komersil digunakan untuk penyaringan pantas keadaan penghabluran yang berpotensi. Pengoptimuman keadaan penghabluran dengan hablur jarum DEPTOR dan DEP12 dilakukan untuk meningkatkan kualiti hablur untuk difraksi sinar-X. Berdasarkan penyerakan cahaya dinamik, DEPTOR, DEP2 dan DEP12 wujud sebagai dimer sementara DEP1 wujud sebagai multimer. Hasil ini menunjukkan bahawa domain DEP mungkin memainkan peranan penting dalam dimerisasi DEPTOR. Tiga model separa yang mewakili setiap domain DEPTOR diramalkan dengan kaedah pemodelan homologi menggunakan SWISS-MODEL. Lukisan skematik kompleks DEPTOR-mTOR dibina berdasarkan ciri

DEPTOR dan struktur mTOR. Dua domain PDZ dimer DEPTOR mengikat secara bebas sebagai monomer ke domain FAT dari mTOR dimerik dengan domain DEP yang terletak di luar mTOR.

## CHARACTERISATION AND CRYSTALLISATION OF DEPTOR

### ABSTRACT

The mechanistic target of rapamycin (mTOR) signalling pathway integrates wide varieties of nutrients to regulate important cellular processes related to cell growth. mTOR is a huge serine/threonine protein kinase and exists in two distinct complexes, mTORC1 and mTORC2. DEPTOR is an endogenous inhibitor of mTOR and consists of two DEP domains in tandem arrangement and a PDZ domain. The *Escherichia coli* expression system was used for cloning and expression experiments. Here, besides the full-length protein, various truncated mutants were designed as well to gain insights into the characteristics and architectures of the protein. Four truncated mutants were constructed to represent the first DEP domain (DEP1), the second DEP domain (DEP2), both DEP domains (DEP12) and the PDZ domain. DEPTOR, DEP1, DEP2 and DEP12 were expressed as soluble proteins but PDZ was insoluble. The soluble proteins were purified to homogeneity for crystallisation through metal-ion affinity purification and size exclusion chromatography. Commercial crystallisation kits were utilized for rapid screening of potential crystallisation conditions. Optimization of crystallisation conditions with needle crystals of DEPTOR and DEP12 were performed to improve the crystal quality for X-ray diffraction. Based on dynamic light scattering, DEPTOR, DEP2 and DEP12 exist as a dimer while DEP1 exists as multimers. These results suggest that the DEP domains probably play a key role in the dimerization of DEPTOR. Three partial models representing each domain of DEPTOR were predicted by homology modelling method using SWISS-MODEL. A schematic drawing of DEPTOR-mTOR complex was built based on the DEPTOR's characterisation and the structure of

mTOR. The two PDZ domains of a DEPTOR dimer bind independently as monomers to the FAT domains of the dimeric mTOR with the DEP domains situated outside of the mTOR.



# CHAPTER 1

## INTRODUCTION

### 1.1 Introduction

Mechanistic target of rapamycin (mTOR) is a serine/threonine protein kinase that belongs to phosphatidylinositol 3-kinase-related kinases (PIKK) family. mTOR acts as the central node to regulate a wide variety of fundamental cellular and metabolic processes through two types of functionally distinct protein complexes known as mTOR Complex 1 (mTORC1) and mTOR Complex 2 (mTORC2) (Dey *et al.*, 2016; Saxton and Sabatini, 2017). mTORC1 promotes cell growth and differentiation through protein synthesis, lipid synthesis, and anabolic metabolism, and inhibits catabolic processes like autophagy while mTORC2 plays an important role in cell survival, proliferation, maturation, and organization of actin cytoskeleton. These complexes integrate a wide variety of nutrients, amino acids, growth factors and stress statuses to modulate wide spectrum of downstream effectors in response to the need of the cells (Kennedy and Lamming, 2016; Saxton and Sabatini, 2017).

The dysregulation of the components in the mTOR signalling pathway often causes major human diseases such as neurodegeneration, type 2 diabetes, obesity and cancer (Dey *et al.*, 2016). Therefore, there has been a rapid rise of ongoing efforts to identify and to study the components of mTOR complexes for potential therapeutic applications (Abdel-Maksoud *et al.*, 2019). A novel mTOR-interacting protein, termed DEPTOR was recently identified as an indispensable component of both mTOR complexes. DEPTOR consists of two DEP domains, a linker and a PDZ domain. Thirteen phosphorylation sites are present on the linker along with a consensus binding site for degradation by proteasome. The PDZ domain of DEPTOR

binds to the FAT domain of mTOR and endogenously inhibits the kinase activities of both mTOR complexes (Peterson *et al.*, 2009).

DEPTOR's activity appears to be largely regulated transcriptionally and post-translationally through complex mechanisms mediated by the mTOR complexes. In most human tumours, DEPTOR expression has been found to be down regulated while mTOR kinase activity is hyperactivated. However, in certain tumour type like multiple myeloma cells, DEPTOR is greatly overexpressed to prevent apoptosis of the cancerous cells (Peterson *et al.*, 2009). These findings suggest that DEPTOR operates in a bifunctional way, as oncosuppressor or as oncogenic factors depending on the type of tumour cells. While there are many literatures on the significance of DEPTOR in the mTOR signalling pathway, there is not much fundamental information on the structure of the DEPTOR-mTOR complex. Here, we aimed to characterise DEPTOR and its truncated mutants (DEP1, DEP2 and DEP12) to gain more insight into the DEPTOR-mTOR complex interactions.

## **1.2 Research Objectives**

- To produce homogenous recombinant DEPTOR, DEP12, DEP1, DEP2 for crystallisation.
- To characterise DEPTOR, DEP12, DEP1, DEP2 through size-exclusion chromatography and dynamic light scattering.

## CHAPTER 2

### LITERATURE REVIEW

#### 2.1 mTOR

mTOR interacts with various regulatory proteins to form two discrete complexes called mTORC1 and mTORC2. These complexes are known for regulating many important cellular biosynthetic processes like growth, division, proliferation, migration, survival, metabolism, autophagy, and angiogenesis (Kennedy and Lamming, 2016; Saxton and Sabatini, 2017). mTORC1 promotes protein synthesis through the phosphorylation of two important downstream targets, 70S6 Kinase1 (S6k1) and the eIF4E-Binding Protein1 (4E-BP1) (Hay and Sonenberg, 2004). Phosphorylated S6K1 activates several critical substrates to induce protein synthesis and to amplify the translation efficiency of newly spliced mRNA (Holz *et al.*, 2005). Phosphorylated 4E-BP1 helps to promote cap-dependent translation at 5' cap mRNA (Ma *et al.*, 2008).

mTORC1 helps to promote the expression of essential glycolytic enzyme such as phospho-fructokinase (PFK). Besides that, mTORC1 also aids in the formation of active Sterol Responsive Element Binding Protein (SREBP) which are essential for promoting cell growth and cell proliferation. De novo lipid synthesis is also promoted by mTROC1 signalling through the SREBP transcription factors that control the expression of genes relevant to cholesterol and fatty acid biosynthesis (Düvel *et al.*, 2010; Mao and Zhang, 2018). In addition to the various mTORC1-anabolic processes described above, mTORC1 also facilitates cell growth by suppressing catabolism process like autophagy.

While mTORC1 regulates cell growth positively, mTORC2 instead is involved in regulating actin cytoskeleton formation and cellular proliferation. The first downstream target discovered for mTORC2 was Protein kinase C alpha (PKC $\alpha$ ), a member of Protein Kinase C (PKC) family. mTORC2 phosphorylates and activates PKC $\alpha$  to regulate actin cytoskeleton organization (Jacinto *et al.*, 2004). Further biochemical analysis of the mTORC2 pathway revealed that mTORC2 was also targeting various members of the PKC family for phosphorylation, driving cytoskeletal reorganization and relocation of cells (Gan *et al.*, 2012; Li and Gao, 2014).

The most well-documented role of mTORC2 is the phosphorylation and activation of Protein kinase B (Akt). Akt is a crucial effector of insulin/PI3K signalling that confer cell survival, proliferation, and growth through the phosphorylation and inhibition of several critical substrates (Sarbasov *et al.*, 2005). Besides that, mTORC2 also phosphorylates Glucocorticoid-Induced Protein Kinase1 (SGK1), a key regulator for ion transport and cellular growth (García-Martínez and Alessi, 2008).

### **2.1.1 Structure of mTOR**

mTOR is a member of phosphatidylinositol 3-kinase-related kinases (PIKK) family, which includes Ataxia-Telangiectasia Mutated (ATM), Transactivation/Transformation domain-associated protein (TRRAP), Ataxia Telangiectasia and Rad3 Related (ATR), Suppressor of Morphogenesis in Genitalia (SMG-1) and DNA-dependent Protein Kinase catalytic subunit (DNA-PKcs). The proteins of the PIKK family are involved in a wide range of cellular functions, ranging from cell proliferation, DNA repair, cell differentiation to embryonic

development (Keith and Schreiber, 1995; Baretic and Williams, 2014). mTOR is a large protein kinase that starts with HEAT repeats domains, which are further subcategorized as N-terminal HEAT repeats (N-HEAT) and middle HEAT repeats (M-HEAT). These domains are then followed by two most crucial domains: the FAT domain and the kinase domain (Yang *et al.*, 2016).

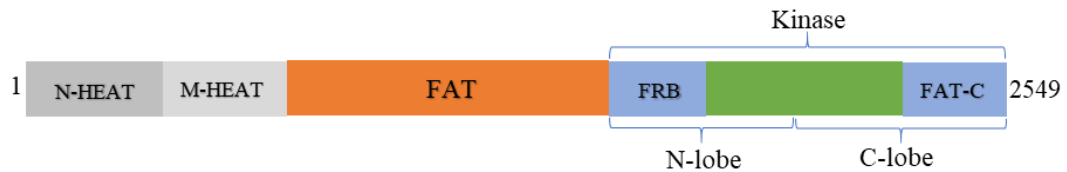


Figure 2.1 Linear schematic of mTOR structure (1-2549 aa).

### 2.1.1(a) FAT domain

mTOR has an N-terminal region known as FAT domain (named after FKBP12-rapamycin-associated protein (FRAP)-ATM-TRRAP) and a short FAT-C domain at the C-terminal region (Bosotti *et al.*, 2000). FAT domain (~600 residues) is made up of three tetratricopeptides repeat-containing protein (TRD1, TRD2, TRD3) and a HEAT-repeat domain (HRD). It forms a C-shaped or also known as  $\alpha$  solenoid that wraps around the kinase domain, promoting interaction between TRD1-kinase domain and HRD-kinase domain through conserved residues. These interactions provide structural stability and catalytic function to mTOR (Yang *et al.*, 2013). Mutation of the conserved residues within FAT domain have been shown to cause hyperactivation of mTOR and enhanced cell proliferation, which eventually leads to cancerous growth (Murugan *et al.*, 2013; Ghosh *et al.*, 2015).

### 2.1.1(b) Kinase domain

The KD (~550 residues) of mTOR takes on a two-lobe structure that consists of C-terminal lobe (N lobe) and a larger C-terminal lobe (C lobe). A ~100 residues domain known as FKBP12-rapamycin binding (FRB) domain forms a protruding insertion in the N lobe. FRB aids in the recruitment of substrate (S6K1) and limiting substrates access into the active site of kinase domain. On the other hand, the C lobe contains four significant structural insertions known as Lst8-binding element (LBE),  $\kappa\alpha$ AL,  $\kappa\alpha$ 9B, and FATC. LBE (~40-residues) acts as a binding site for mLST8, a key component for stabilizing kinase domain.  $\kappa\alpha$ 9B (~11 residues) also prevents substrate access into the active site of kinase domain. The FAT-C (~35 residues) insertion forms a helix that interacts with LBE and another three helices that interact with the activation loop of kinase domain. Activation loop is a well-ordered region that plays a crucial role in the functioning and regulation of mTOR. The interactions that FAT-C make with LBE and activation loop are thought to provide structural stability for the kinase domain (Yang *et al.*, 2013; Baretic *et al.*, 2016; Chao and Avruch, 2019).

The presence of structural insertions on N lobe and C lobe produce a V-shaped structural cleft that acts as binding site for ATP for phosphorylation of substrates. This V-shaped cleft also restricts the entry of substrate to the active site of kinase domain from the bottom of the cleft. There are multiple conserved core residues on the active site of kinase domain, which are essential for regulation of mTOR. For example, Asn2343 and Asp2357 can be found on the C-lobe, and they serve as binding sites for metal ligand while Asp2338 is crucial for nucleophilic attack. Besides that, mutation of His2340 causes inactivity of mTOR's kinase, revealing the significance of this residue (Yang *et al.*, 2013).

## 2.2 DEPTOR

A novel DEP domain-containing protein was discovered in mammalian cells during immunoprecipitation of mTOR (Peterson *et al.*, 2009). Further analysis showed that this protein can interact with mTOR and was named as DEPTOR (Peterson *et al.*, 2009). It consists of three highly conserved domains: two DEP domains in tandem at the N-terminal region and a PDZ domain at the C-terminal region. Multiple phosphorylation sites are present on the linker region, which are situated between the C-terminal DEP domain and the PDZ domain for the regulation of this protein activity (Peterson *et al.*, 2009). Importantly, it negatively regulates mTOR activities by binding to the FAT domain of mTOR through its PDZ domain, causing suppression of mTOR's kinase phosphorylation activities (Chen and Hamm, 2006; Peterson *et al.*, 2009). Besides regulating mTOR, DEPTOR is also shown to be involved in regulating several molecular processes such as autophagy and cell survival (Zhao *et al.*, 2011; Srinivas *et al.*, 2016).



Figure 2.2 Schematic structure of DEPTOR.

### 2.2.1 Biological functions of DEPTOR

Various studies have shown that DEPTOR is a positive regulator of autophagy pathway (Zhao *et al.*, 2011; Zhang *et al.*, 2013). Autophagy is a tumour suppressing process which degrades damaged cell contents and proteins that are susceptible to aggregation in lysosome (Glick *et al.*, 2010). When a cell is exposed to low-energy state due to glucose shortage, mTOR inactivates and DEPTOR accumulates to induce autophagy. The onset of autophagy induced by DEPTOR can

be confirmed by the accumulation of microtubule-associated protein 1A/1B-light chain 3 (LC3-II) proteins in the energy-deprived cell (Zhao *et al.*, 2011). Autophagy helps to protect and provide energy for the cells by degrading damaged cell contents and proteins that are susceptible to aggregation in lysosome (Glick *et al.*, 2010).

Furthermore, DEPTOR can also promote cell survival in tumour cells. In cervical squamous cell carcinoma (SCC), overexpression of DEPTOR is necessary for PI3K/AKT pathway to confer proliferative and survival advantage to the tumour cells (Srinivas *et al.*, 2016). In this regard, sustained activation of PI3K/AKT signalling is common and necessary in certain cancer to ensure favourable growth environments for the tumour cells (Dey *et al.*, 2016). In agreement, knockdown of DEPTOR prevents activation of PI3K/AKT pathway and this leads to cell death via complex signalling pathways involving down-regulation of PI3K/AKT by mTORC1-S6k1 and up-regulation of p38 mitogen-activated protein kinase (MAPK) (Srinivas *et al.*, 2016).

### **2.2.2 DEPTOR regulation**

DEPTOR, an endogenous inhibitory protein of mTOR, is degraded through proteasome-dependent degradation (Duan *et al.*, 2011; Gao *et al.*, 2011). The E3 ubiquitin ligase, SCF (Skp1-Cul1-F-box) complex is involved in the ubiquitination and degradation of DEPTOR (Zhao *et al.*, 2011). SCF complex is made up of SKP1 (S-phase Kinase-associated Protein 1), Cullins,  $\beta$ TrCP (F Box protein) and a RING protein, RBX (RING Box protein (Zhao *et al.*, 2011). The linker region of DEPTOR contains the consensus binding site (degron site), SSGYFS and phosphorylation on Ser286, Ser287, Ser293, Ser299 in the degron is necessary before it can be recognized by  $\beta$ TrCP for ubiquitination and degradation by SCF



complex (Duan *et al.*, 2011; Gao *et al.*, 2011; Zhao *et al.*, 2011). Upon growth stimulation, mTOR phosphorylates DEPTOR at Ser293 and Ser299 residues to promote further phosphorylation by casein Kinase1 (CK1) at Ser286 and Ser287 residues (Duan *et al.*, 2011; Gao *et al.*, 2011). These phosphorylation events drive the formation of phosphodegron on DEPTOR that binds to the  $\beta$ TrCP (Gao *et al.*, 2011). Hence, DEPTOR is subjected to negative regulation by  $\beta$ TrCP through phosphorylation dependent degradation.

In addition, there is another mechanism that has been reported to dissociate DEPTOR from mTOR without the involvement of its phosphorylation. In the presence of mitogens, phosphatidylcholine (PC) is hydrolysed by phospholipase D (PLD) to phosphatidic acid (PA). PA is able to relieve DEPTOR's binding on mTOR in a rapid manner by associating with the FRB domain of mTOR (Yoon *et al.*, 2015).

### **2.2.3 DEP domain**

DEP domain is a conserved domain of ~100 residues that were initially apparent in three different proteins: Dishevelled, EGL-10, and Pleckstrin (Ponting and Bork, 1996; Kharrat *et al.*, 1998; Civera *et al.*, 2005). Dishevelled (DVL), egg-laying defective protein 10 (EGL-10) and Pleckstrin were first discovered in the common fruit fly, *Caenorhabditis elegans* and mammalian cells, respectively (Ponting and Bork, 1996; Kharrat *et al.*, 1998; Civera *et al.*, 2005). Later, the acronym DEP (from the initial letters of DVL, EGL-10 and Plecksrin) was adopted by the scientific community (Ponting and Bork, 1996; Kharrat *et al.*, 1998; Civera *et al.*, 2005). Presently, there are also other proteins with DEP domain, including the regulator of G protein signalling (RGS) family of proteins, exchange protein directly activated by cAMP (EPAC), and PtdIns(3,4,5)P<sub>3</sub>-dependent RAC exchanger (PREX)

(Consonni *et al.*, 2014). Extensive structural analysis has shown that DEP domain has characteristic of  $\alpha/\beta$  fold, consisting of several  $\alpha$ -helixes and a protruding  $\beta$ -hairpin arm. The residues in the helical structures are quite conserved among the DEP domain-containing proteins. In contrast, the residues in the  $\beta$ -hairpin structure are less conserved, as this part is involved in performing diverse functions during signal transduction events (Axelrod *et al.*, 1998; Wong *et al.*, 2000; Civera *et al.*, 2005).

DEP domain is a globular protein module that primarily functions to assist protein translocation to plasma membrane through membrane binding but also carrying out different function like assisting in protein complex formation. For DVL, its DEP domain helps to anchor its protein to the plasma membrane to promote formation of protein complexes, necessary for the regulation of 'Wingless/Integrated' (WNT) signalling pathway (Pan *et al.*, 2004). In the case of RGS family of proteins, the DEP domain has an indispensable helical structure known as DEP helical extension (DHEX). DEP-DHEX domain aids in the membrane anchoring process to other anchoring proteins and this domain also provide a necessary binding interface for protein complexes formations at the cell membrane (Patil *et al.*, 2018). In *Caenorhabditis elegans*, asymmetric cell division is a common occurrence, in which the smaller daughter cell will be broken down by apoptosis. The DEP domain in the target of ERK kinase MPK-1 (TOE-2) protein helps to localize TOE-2 to the membrane of the smaller daughter cell for induction of apoptosis (Gurling *et al.*, 2014).

#### 2.2.4 PDZ domain

The PDZ (postsynaptic density 95, PSD-95; discs large, Dlg; zonula occludens-1, ZO-1) domain is a protein module of ~90 residues, firstly discovered in three proteins known as PSD-95, Dlg, and ZO-1 (Cho *et al.*, 1992; Willott *et al.*, 1993; Nourry *et al.*, 2003). PDZ domain-containing protein is commonly found in a wide range of organisms such as bacteria, common fruit fly, yeast, plants, and humans. It is predominantly involved in mediating protein-protein interactions during signal transduction events and assists in the formation of protein complexes at the plasma membrane (Fanning and Anderson, 1996; Lee and Zheng, 2010). For example, PDZ domain of DEPOR has been reported to bind to mTOR's FAT domain for suppression of mTOR's kinase activities (Peterson *et al.*, 2009). Extensive structural studies by nuclear magnetic resonance (NMR) and X-ray crystallographic methods showed that PDZ domain usually consists of about five to six  $\beta$ -strands and two to three  $\alpha$ -helixes (Cabral *et al.*, 1996; Im, Park, *et al.*, 2003; Kang *et al.*, 2003). PDZ domain usually exists as multiple copies together or with other protein domains but also can occur as single copy alone or with other protein domains as well (Spaller, 2006). Besides that, isolated PDZ domain from its cytoplasmic protein usually forms monomer and dimerization of PDZ domains also occurs but is rare (Cabral *et al.*, 1996; Im, Lee, *et al.*, 2003).

PDZ domain proteins interact with other proteins with specificity in multiple ways. The most well-known way is the binding of PDZ domain directly to the carboxy-terminal of target proteins to assemble protein complexes (Songyang *et al.*, 1997). One example is that the PDZ domain of PSD-95 can bind to the shaker potassium ion channels by recognizing specific amino acid residues at the C-terminal

of its target protein (Kim *et al.*, 1995). Besides, PDZ domain can also bind directly to the internal sequence motifs of the target protein. For example, instead of targeting the C-terminal ligands, the PDZ domain of partitioning defective protein 6 (par-6) protein can directly bind to the internal ligands of protein-containing ALS2cr12 signature (Pals-1) (Penkert *et al.*, 2004). PDZ domain-mediated interactions are often regulated through phosphorylation of PDZ ligand, phosphorylation of PDZ domain itself, and adopting autoinhibitory conformation by PDZ-containing proteins (Chung *et al.*, 2004; Morales *et al.*, 2007; Steiner *et al.*, 2008).

### **2.3 X-ray protein crystallography**

X-ray crystallography is the most favoured method to determine the three-dimensional structure of proteins. X-ray diffraction requires that protein samples be purified to homogeneity and undergo broad crystallisation screening at high protein concentration. Once initial crystallisation conditions are established, it is necessary to further improve the crystal quality by optimizing around the conditions that have led to crystal hits by adjusting the different components in the crystallisation conditions. The improved crystal is then exposed to a finely focused X-ray beam, resulting in the scattering of X-ray caused by the atoms in the crystal and recorded as diffraction spots by a detector. The pattern of the diffracting spots can then be processed and analysed to yield information about the crystal packing symmetry and the size of the repeating unit that forms the crystal. A map of the electron density of the protein is then calculated using one of several methods such as molecular replacement that uses a related structure, or single-wavelength anomalous diffraction (SAD), and the map is used to build the structure of the protein. Besides X-ray crystallography, nuclear

magnetic resonance (NMR) and cryo-electron microscopy (Cryo-EM) can also be used to determine the structure of a protein.

## CHAPTER 3

### MATERIALS AND METHODS

#### 3.1 Cloning by homologous recombination method

In this method, the forward and reverse primers were designed in such a way to produce inserts with ends that overlap with the ends of a linearized vector. The inserts and linear vectors containing overlapping ends are assembled *in vivo* into a recombinant plasmid in *Escherichia coli* cells.

##### 3.1.1 Polymerase Chain Reaction (PCR)

KAPA HiFi HotStart ReadyMix PCR kit (KaPa Biosystem) was used to perform high-fidelity PCR. The PCR reaction was performed in final volume of 20  $\mu$ L. Each tube contained 10-100 ng of template DNA, 10  $\mu$ L of 2X KAPA HiFi HotStart ReadyMix, sterilized water, 0.3  $\mu$ M of the forward primer and 0.3  $\mu$ M of the reverse primer. The PCR tubes were then placed in a Veriti 96-Well thermal cycler (Thermo Scientific, USA). The first step of the PCR reaction was one cycle of initial denaturation (95°C for 3 minutes) and followed by twenty-five cycles of reactions consisting of three steps: denaturation (98°C for 20 seconds), annealing (65°C-72°C for 15 seconds) and extension (72°C for 1 minute per 1 kb). Lastly, the PCR reaction underwent one cycle of final extension (72°C for 1 minute per 1 kb) to finish up the amplification process. The thermal cycler was cooled down to 4°C after the last step of PCR reaction. The annealing temperature, extension duration and final extension duration were adjusted for the different DNA lengths of gene of interests.

### 3.1.2 Restriction Enzyme Digestion

pET-21a(+) (Novagen plasmid #69740) (Appendix O) contains a commonly used purification tag, known as polyhistidine tag (6xHis tag). The target inserts were tagged with 6xHis tag, and the recombinant proteins were expressed via inducible T7 promoter. Restriction digestion of the plasmid DNA was done in 50  $\mu$ L reaction volume. The plasmid DNA to be digested was taken from 100 ng/ $\mu$ L stock. The components were mixed briefly and incubated at 37°C for 2 hours before gel electrophoresis. Table 3.1 contains the reaction components used for plasmid DNA digestion.

Table 3.1 Reaction components used for plasmid DNA digestion.

Reaction components	Volume, $\mu$ L
Sterile water	10.2
FastDigest buffer (10x)	5
BamH1 (1 unit/ $\mu$ L)	1.6
Nde1 (1 unit/ $\mu$ L)	1.6
Xho1 (1 unit/ $\mu$ L)	1.6
Plasmid DNA (3000 ng/ $\mu$ L)	30
Total volume	50

### 3.1.3 DNA Purification

PCR products and digested vectors were purified using GeneJET PCR purification kit (Thermo Scientific, USA). The DNA was mixed with 1 volume of binding buffer, transferred to the GeneJET purification column, and centrifuged for 1 minute at 14000 rpm. The flow through was discarded, and the bound DNA was washed with 700  $\mu$ L wash buffer by centrifugation. After the wash through was

discarded, the column was centrifuged again to remove residual ethanol. The column was then transferred to a clean 1.5 mL Eppendorf tube (Eppendorf, Germany) and the DNA was eluted with 50  $\mu$ L of elution buffer by 1 minute of centrifugation. The concentration of the purified DNA was measured using Nanodrop 2000 (Thermo Scientific, USA).

#### **3.1.4 Agarose Gel Electrophoresis**

Agarose gel solution was prepared by mixing 0.7 % agarose (Lonza, Switzerland) in 30 mL of 1x TAE buffer and was heated in microwave until the solution became clear. Before pouring into the gel tray containing comb teeth, the clear solution was added with 2.5  $\mu$ L of Redsafe Nuclei Acid Staining Solution (20 000X) (Intron, Korea). The DNA samples were mixed in tubes that contained 2.5  $\mu$ L of 100 ng/ $\mu$ L DNA solution and 0.5  $\mu$ L of 6x loading dye. The loaded agarose gel was subjected to 100 volts until the dye reached  $\frac{3}{4}$  of the way down the gel. The gel was visualized in the universal hood II gel doc system (Bio-rad, USA).

#### **3.1.5 Cloning of DEPTOR and its truncated mutants into pET-21a(+)**

The pRK5-Flag human DEPTOR (N204S and S389N; Addgene plasmid #21334) (Appendix P) were purchased from Addgene, USA. The plasmid was used as template for PCR amplification of DEPTOR (Accession No. NM\_022783.4). Online web services like BLAST and PSIPRED were used to assist in the construction of truncated mutant protein. DEPTOR gene was amplified and inserted into pET-21a(+) plasmid. The pET-21a(+)-DEPTOR was employed as template for the amplification of four truncated mutants labelled as DEP1 (DEPTOR domain 1),





### 3.1.6 Correcting mutation at position 611 and 1166

There were two-point (substitution) mutation in the coding sequence of DEPTOR, purchased from Addgene, when translated into amino sequence, conservative missense mutation can be detected at residue position 204 and 389. The mutation is located at nucleotide position 611 and 1166, which represent G (Guanine) and A (alanine) respectively and four primers were designed to correct the mutations: (G to A) and (A to G) (Figure 3.1). Each primer carried the desired correction (nucleotide in bold) to perform single substitution correction. PCR reaction was prepared based on the method described in section 3.1.1. The sequence of corrected DEPTOR was confirmed through DNA sequencing. Table 3.3 shows the list of primers used to correct the mutations. Table 3.4 shows the nucleotide corrections by their respective primers.

Table 3.3 List of primers used to correct the mutations.

No.	Length	Primers (5'-3')
1	41	CATCATCCAGCATGTGTCCA <b>A</b> CAAGCACCCATTTGTGGACA
2	41	TGTCCACAAATGGGTGCTTGT <b>T</b> GGACACATGCTGGATGATG
3	41	TGTAGACTACCGGACCGTGAG <b>G</b> CAATCTGATTCTGACGGGCC
4	41	GGCCCGTCAGAATCAGATTGCTCACGGTCCGGTAGTCTACA

Table 3.4 Nucleotide corrections by their respective primers.

Primers	Nucleotide corrections
Forward primer of DEPTOR and primer no.2	G to A
Primer no.1 and primer no.4	A to G
Primer no.3 and reverse primer of DEPTOR	A to G

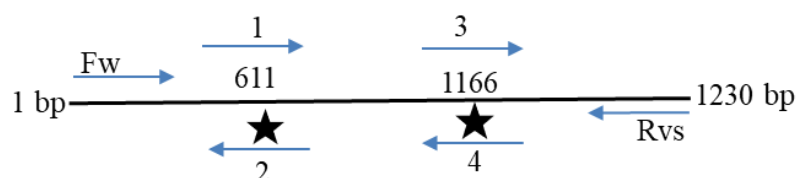


Figure 3.1 Correcting mutation at position 611 and 1166 via PCR. Forward primer of DEPTOR (Fw) and primer no.2 underwent PCR reaction to produce the first fragment. Primer no.1 and primer no.4 underwent PCR reaction to produce the second fragment. Primer 3 and reverse primer of DEPTOR (Rvs) underwent the last PCR reaction to produce the third fragment. They were combined in one final PCR reaction with Fw and Rvs as primers.

### 3.1.7 Identification and optimization of rare codons in DEPTOR

Using online website ([https://www.bioline.com/media/calculator/01\\_11.html](https://www.bioline.com/media/calculator/01_11.html)), the position of tandem and triple rare codons were identified. Three tandem rare codons and one triple rare codons were optimized to frequently used codons reflective of *E. coli* codon system. The primers used contained the desired codons (nucleotide in bold) for multiple sites substitution mutagenesis via PCR. A total of six primers were used in the optimization of rare codons of DEPTOR as shown in Figure 3.2. PCR reactions were prepared based on the method described in section 3.1.1. The sequence of codon optimized DEPTOR was confirmed through DNA sequencing. Table 3.5 shows the position of rare codons and their corresponding amino acids. Table 3.6 shows the lists of primers used to remove the rare codons and replace frequently used codons. Table 3.7 shows the rare codon optimization by their respective primers.

Table 3.5 Position of rare codons and their corresponding amino acids.

Position of rare codons	Rare codons
138, 139	Arginine (AGG), Leucine (CUA)
153, 154	Proline (CCC), Arginine (AGG)
277, 278	Arginine (AGG), Arginine (AGA)
225, 226, 227	Arginine (AGG), Arginine (CGA), Arginine (AGA)

Table 3.6 Lists of primers used to optimize the rare codons in DEPTOR.

No.	Length	Primers (5'-3')
1	60	Reverse: GGAGTGTGTTTTCAGGGCTCATCAGCTTTTCATAAAGACGCT GTCCCTCATAAAGGCCT
2	60	Forward: AAAGCTGATGAGCCCTGAAAACACACTCCTGCAGCCGCGCG AGGAGGAAGGGGTCAAGTA
3	49	Reverse: GCTCCATCAGGCGGCGGCGCCGCCGGAAGTTCATTCTGAAC TGGTAGAG
4	49	Forward: CTTCCGGCGGCGCCGCGCCTGATGGAGCTGCTCAATGAAA AGTCCCCC
5	49	Forward: CGTGTCTGCAGTGCCTCGTAGCAGCATGAGCAGCTGTGGCA GCAGCGGC
6	49	Reverse: TGCTCATGCTGCTACGACGCACTGCAGACACGATCTTGATCT CCTTGCT

Table 3.7 Rare codon optimization by their respective primers.

Primers	Rare codon optimization
Forward primer of DEPTOR and primer no.1	AGGCUA to AAGAGC
Primer no.2 and primer no.3	CCCAGG to CCGCGC
Primer no.4 and primer no.6	AGGCGAAGA to CGCCGCCGC
Primer no.5 and reverse primer of DEPTOR	AGGAGA to CGTCGT

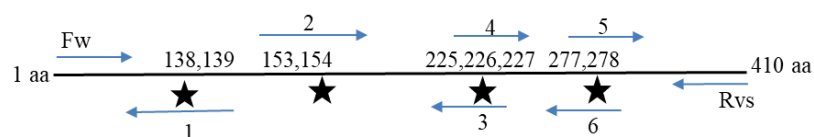


Figure 3.2 Optimization of rare codons via PCR. Forward primer of DEPTOR (Fw) and primer no.1 underwent PCR reaction to produce the first fragment. Primer no.2 and primer no.3 underwent PCR reaction to produce the second fragment. Primer no.4 and primer no.6 underwent PCR reaction to produce the third fragment. Primer no.5 and reverse primer of DEPTOR (Rvs) underwent the last PCR reaction to produce the fourth fragment. They were combined in one final PCR reaction with Fw and Rvs as primers.

### 3.2 General transformation of *E. coli* for cloning

The *E. coli* strains DH5 $\alpha$  (Thermo Fisher Scientific, cat#18265017) was used for cloning. A 1.5 mL Eppendorf tube containing chemically competent DH5 $\alpha$  *E. coli* cells was thawed on ice for 5 minutes. Then, the purified DNA (PCR products and digested vector) were added in a ratio of 1:3 into the competent cell tube. In the case of transforming plasmid/vector only for propagation, 1  $\mu$ L of 100 ng/ $\mu$ L plasmid/vector was added into competent cells. After that, the tube was incubated on ice for 30 minutes before heat shocked at 42°C for 45 seconds. Then, 700  $\mu$ L of LB broth was added into the tube and incubated at 37°C for 1 hour with shaking. After incubation, the mixture was centrifuged at 14000 rpm for 1 minute using tabletop centrifuge 5418 (Eppendorf, Germany). The supernatant was briefly decanted, and the leftover supernatant was used to resuspend to pellet. The cell suspension was plated on LB agar plate containing ampicillin and incubated at 37°C overnight.

#### 3.2.1 Transformation of *E. coli* with recombinant vector for expression

Recombinant vector (100ng/ $\mu$ L) was added into the thawed, chemically competent BL21(DE3) (Novagen, cat #69450) / Lemo21(DE3) (NEB, cat #C2528J) /

NiCo21(DE3) (NEB, cat #C2529H). The rest of the methods described in section 3.2 were applied here except during the plating. For Lemo21(DE3), LB agar plates containing ampicillin and chloramphenicol were used.

### **3.2.2 Transformation of *E. coli* with rare tRNA-supplying plasmid**

NiCo21(DE3) was transformed with rare tRNA-supplying plasmids called pRARE2 (Novagen) and pACYC-RIL (Novagen). After thawing, 1  $\mu$ L of 100 ng/ $\mu$ L plasmid was added into chemically competent NiCo21(DE3) and followed by methods, described in section 3.2 except during plating. The cell suspension was plated on LB agar containing chloramphenicol since the rare tRNA-supplying plasmid also has its own resistant marker. At the end, three types transformants were produced and they were called as NiCo21(DE3)-pRARE2, NiCo21(DE3)-pACYC-RIL and NiCo21(DE3)-pRARE2, pACYC-RIL. These transformants were cultured and chemically turned into competent cells.

### **3.2.3 Transformation of NiCo21(DE3)-tRNA plasmid with recombinant vector**

pET-21a(+) containing corrected and codon optimized DEPTOR gene was transformed into each of the chemically competent NiCo21(DE3)-pRARE2, NiCo21(DE3)-pACYC-RIL and NiCo21(DE3)-pRARE2, pACYC-RIL. They were plated on LB agar plate containing ampicillin and chloramphenicol.

### **3.3 Colony PCR and plasmid isolation**

Colony PCR method was employed to screen for the absence and presence of insert in the plasmid constructs. Five colonies on the LB agar plate containing

ampicillin were selected for testing. Each of the colonies was picked up using clean 10  $\mu$ L pipette tip and mixed thoroughly in the PCR tube containing 10  $\mu$ L of sterile water. The tubes were then boiled at 95°C using the thermal cycler. In the meantime, PCR master mix containing the appropriate volume of all reaction components were prepared. The master mix was aliquoted out to their individual PCR tubes. The boiled tubes were then centrifuged for 1 minute at 14000 rpm using tabletop centrifuge 5418 (Eppendorf, Germany). One  $\mu$ L of supernatant was taken as template to amplify the inserts during twenty-five PCR cycles with KAPA HiFi HotStart ReadyMix. Positive clones were detected through gel electrophoresis and confirmed through DNA sequencing.

### **3.4 Protein expression**

#### **3.4.1 Small-scale protein expression using recombinant pET-21a(+)**

Expression parameters such as solubility and expression levels were analysed and identified for a given target through these small-scale expression cultures. The LB agar plate containing transformed colonies were picked up and inoculated into the initial 5 mL LB culture supplemented with 100  $\mu$ g/mL ampicillin for overnight incubation at 37°C. On the following day, a 50 mL LB broth supplemented with 100  $\mu$ g/mL ampicillin, was inoculated with 500  $\mu$ L of the initial culture. The bacterial cells were cultured for about 2 to 3 hours at 37°C with 200 rpm agitation until the OD<sub>600</sub> reached 0.6-1.0 OD. One mL of culture was transferred out to be analysed as uninduced fraction. After that, the remaining culture was induced with IPTG with a range of final concentrations of 0.1 - 1 mM. The culture was then incubated at 25°C overnight (16 hours).

BL21(DE3) was used as the expression host for the expression of DEPTOR, DEP12, DEP1 and DEP2. In some experiments, Lemo21(DE3) were being used as expression hosts, therefore, 100 µg/mL ampicillin and 40 µg/mL chloramphenicol were added into the cultures. For Lemo21(DE3), different concentrations of rhamnose were also added into the cultures to control the expression of the recombinant protein.

### **3.4.2 Small-scale expression of DEPTOR in NiCo21(DE3)**

NiCo21(DE3) is a derivative of BL21(DE3), engineered to minimize the contamination of endogenous *E. coli* proteins in IMAC fractions. In NiCo21(DE3), the glutamine-fructose-6-phosphate aminotransferase (glms) gene is mutated to remove the binding of *E. coli* contaminating protein to nickel resins. Since NiCo21(DE3) is beneficial for large-scale IMAC purification stage, corrected and codon optimized DEPTOR was expressed in NiCo21(DE3). The small-scale cultures were tested first, and the expressions were performed based on the method described above (Section 3.4.1).

### **3.4.3 Small-scale expression of DEPTOR with rare tRNA-supplying plasmid**

The expression of corrected and codon optimized DEPTOR was performed in chemically competent NiCo21(DE3)-pRARE2, NiCo21(DE3)-pACYC-RIL and NiCo21 (DE3)-pRARE2, pACYC-RIL. The small-scale cultures were grown with both antibiotics (100 µg/mL ampicillin and 25 µg/mL chloramphenicol) and the expressions were performed based on the method described above (Section 3.4.1).